

Chapter

Assessing the Impact of Spectral Irradiance on the Performance of Different Photovoltaic Technologies

*Mohammad Aminul Islam, Nabilah M. Kassim,
Ammar Ahmed Alkahtani and Nowshad Amin*

Abstract

The performance of photovoltaic (PV) solar cells is influenced by solar irradiance as well as temperature. Particularly, the average photon energy of the solar spectrum is different for low and high light intensity, which influences the photocurrent generation by the PV cells. Even if the irradiance level and the operating temperature remain constant, the efficiency will still depend on the technological parameters of the PV cell, which in turn depends on the used PV material's absorption quality and the spectral responsivity and cell structure. This study is devoted to the review of different commercially available technologies of PV cells include crystalline silicon (c-Si), polycrystalline silicon (pc-Si), cadmium telluride (CdTe), and copper indium gallium selenide (CIGS). We tried to correlate the spectral response or the photocurrent of different PV cells with the variations of the solar spectrum, environmental conditions, and the material properties and construction of PV cells.

Keywords: photovoltaics technology, average photon energy, spectral irradiance, spectral effect, photovoltaic performance

1. Introduction

The energy demand is increasing concurrently with the increase of the world's population and meeting the increasing energy demands including managing social, economic, and ultimate environmental issues are one of the greatest challenges of the present time. Solar energy, as one of the promising renewable energy sources, is becoming an important source of energy all over the world. Its huge development potential has attracted a lot of attention and the photovoltaic (PV) industry has been experiencing a large-scale development to replace traditional energy. Also, a significant increase in energy conversion efficiency and the decrease in the price of the solar panels along with various national policies over the world enhanced the solar PV-based energy generation with the least Levelized-cost-of-energy (LCOE). However, for getting optimum output, proper resource estimation is necessary to assess the feasibility of solar PV systems in any area. The output of any PV system's output indeed depends on the weather of its surroundings will be elaborated in this chapter.

In contrast, there are several types including different technologies of photovoltaic modules in the market. However, the technological choices are very critical in the sense of the lack of guide and forecasting tools suited to the climates and environment of the installation sites. There have been many PV system projects going to fail due to the bad choice of PV technology where failure causes are influenced by the environmental parameters, such as heat, humidity, shadow, and dust, etc. Manufacturers provide a characteristic of PV modules measured in standard test conditions (STC), however, the performance cannot reach that level in real operating conditions. Besides, the PV module's performances and aging strongly depend on the climate and the surrounding environment of the installation site.

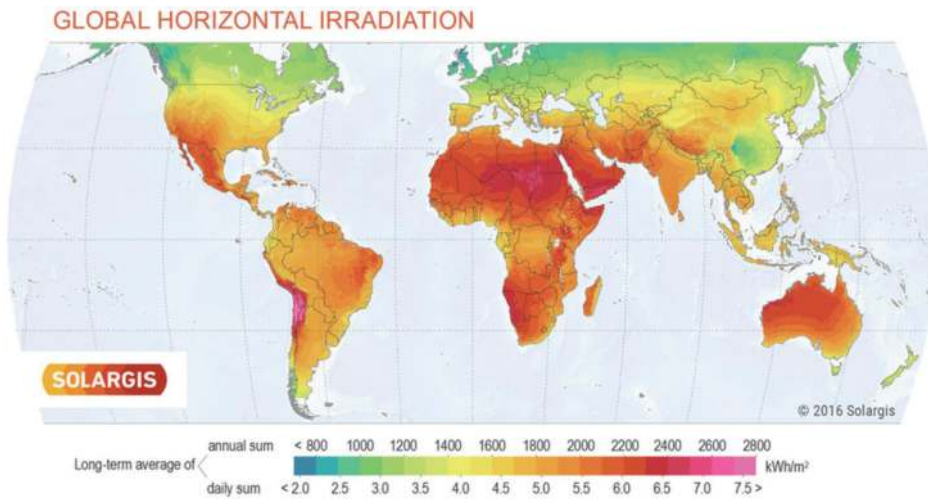
The investigation of PV performance under real external conditions became an important factor as a result of increasing trends of PV capacity over the world. Particularly, the performance of the PV module influence by the number of different external issues, such as, (i) spectral irradiance, i.e., the wavelength of incident light and light intensity, the efficiency of PV certainly varied with the variations in the spectrum of sunlight [1–4] and light intensity directly affect the short circuit current [5]; (ii) reflectivity of the module surface, however, the reflectivity that occurred in the module surface depends on the angle between the module surface and the incident angle [6]; and (iii) module temperature, particularly temperature of the module surface increases to 60-80 °C at noon and cause of the reduction in open-circuit voltage which also depend on the light intensity and airflow [7]. Thus, in each PV field, the factors that contribute to solar cell efficiency are different and the important considerations applied in each area are different. On the other hand, some types of PV modules show the degradation of power conversion efficiency under the long-term light exposer in the field and/or elevated temperatures. Particularly, due to the above-mentioned effects, the module efficiency and/or electrical parameters are observed to deviate from the nameplate value measured under Standard Test Conditions (STC) [8] in the real external condition. Besides, there are some other causes for which the energy production capability of a PV module is affected, such as installation angle; possible shadow, dust or snow deposition, etc. However, these mostly depend more on the details of the installation, not inherent to the module type and the physical properties of the module. It could be mention that the power output could vary as an impact of the above-listed causes while different types of the module installed in the same way; alternatively, similar types of module generate different power output due to the installation in a different way or different places. The variation of PV performance has been investigated by several authors in terms of geographical variability and technology. Some authors only focused on the effect of solar irradiation while other authors consider some of the above-mentioned factors. In this study, we also only reviewed the study that focuses on the effect of solar irradiance on the different PV technology.

2. Spectrum irradiance on earth surface

Solar irradiance on different locations of the earth is shown in **Figure 1** [9]. The maps highlight the global horizontal irradiation (GHI) which means that the overall irradiance from the sun reaches the earth's horizontal surface. It is related to the diffuse horizontal irradiance (DHI) and direct normal irradiance (DNI) as follows [10],

$$GHI = DHI + DNI \times \cos\theta \quad (1)$$

Where θ is the solar zenith angle. Areas with a high proportion of GHI include South-East China, Northern Europe, and the tropical belt around the equator.



[100] World Bank. 2017. Global Solar Atlas. <https://globalsolaratlas.info>

Figure 1.
Global horizontal irradiation (GHI) over the world [9].

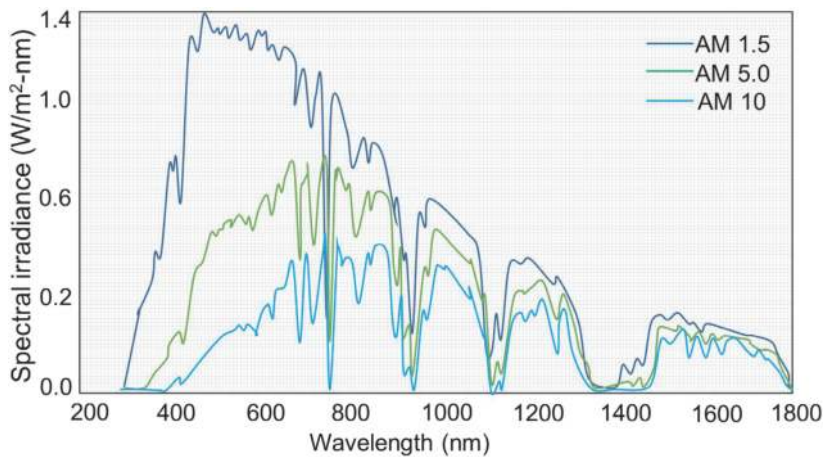


Figure 2.
Impact on the direct spectral irradiance of air mass (AM) simulated with the SMARTS model [11].

Since the electrical performance of PV devices is greatly affected by the incident light spectrum, hence, significant efforts have been given by the PV community to develop methods and evaluate the impact of the spectral variations on the PV device performance over the last three decades. The parameters that have the highest impact on the spectrum distribution as well as on the PV module performance are (i) the air mass (AM), (ii) the perceptible water (PW), and (iii) the aerosols optical depth (AOD) [11].

The AM is a measure of the atmospheric absorption that affects the spectral content and the intensity of the solar radiation coming to the earth's surface. The impact of AM on the solar spectral distribution is shown in **Figure 2** [11]. Particularly, the solar spectral distribution just above the Earth's atmosphere—in the relative vacuum of space is commonly referred to as an air mass zero (AM0). And the AM = 1.0 at sea level when the sun is directly overhead (zenith angle, $\theta_z = 0$). As the θ_z increases, the path passes by the sun spectrum through the atmosphere become

longer, and AM increases. The AM could estimate simply using a trigonometric function of the zenith angle:

$$AM = \frac{1}{\cos \theta_z} = \sec \theta_z \quad (2)$$

where θ_z is the angle of incidence or solar zenith angle.

The above equation is quite accurate for $\theta_z \leq 80$ degrees, however, more complex and precise models are necessary when the sun goes near the horizon. Moreover, the distribution of the outdoor solar spectrum varied during the day due to the presence of water vapors and aerosol in the air. Thus, the real spectrum at the earth's surface is infrequent to fit with the AM1.5 standard solar spectrum as defined in standard IEC 60904-3 and/or ASTM GE173-03 [12]. Specifically, the spectral power distribution observed in the sun at an angle of about 48.2° is specified as AM 1.5 spectrums (as in **Figure 3(a)**). The power density of AM1.5 light is about $1,000 \text{ W/m}^2$. The standard AM 1.5 spectrum is known as solar constant and is normally used in solar cell analysis. **Figure 3(b)** shows the spectral distribution of sunlight under the different air masses.

Another important parameter that needs to be considered for understanding solar irradiance on the earth's surface is the clearness index (K_T). Particularly, K_T is defined by the ratios of the solar radiation for a particular day and the extraterrestrial solar radiation for that day. It could also be defined by hourly as shown below:

$$K_T = \frac{H}{H_o} \text{ (daily) and } k_T = \frac{I}{I_o} \text{ (hourly)} \quad (3)$$

Where H and I represent the total measured and H_o and I_o are represent the extra-terrestrial solar radiation which could be calculated using several approaches [14]. This value of K_T or k_T lies between zero and one which contingent on atmospheric conditions. For clear sky conditions, K_T is near 1 and if the sky is very cloudy and/or turbid and/or heavily overcast, K_T becomes less than 0.4. Several laboratories have been developed computational models considering spectral direct beam during the clear sky and hemispherical diffused irradiances on a surface either horizontal or tilted condition for a certain location and time [15]. Other than the above parameters, the outdoor energy yield and performance of the PV modules further depend on a large number of on-site factors or local factors such as ambient temperature, wind, and rain. These undefined factors may also influence significantly amount of solar radiation that arrives on the surface of the PV module.

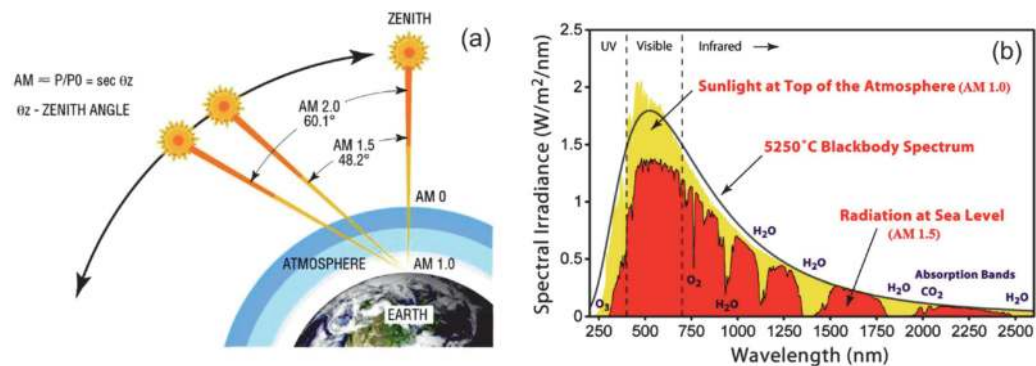


Figure 3. (a) The path length (in units of air mass) changes with the zenith angle (b) spectral distribution of solar energy [13].

Certainly, it is important to analyze the influences of all the above on-site environmental factors on the outdoor performance of different types of PV modules, for finding out the best-suited technology for a specific location and enabling more widespread deployment.

3. PV performance parameters and spectrum

3.1 PV performance parameters

The electrical power generated in a solar cell or PV device can be modeled with a well-known equivalent circuit as shown in **Figure 4** which includes a shunt resistance parallel with a diode and a series resistance [16].

This equivalent circuit can be used for either an individual cell, a multi-cell module, or an array consisting of multiple modules. Using this model and considering constant temperature and solar radiation, the current-voltage equation for a solar cell or module could be expressed as shown in Eq. (4).

$$I = I_0 \left[\exp \left(\frac{qV}{A} \right) - 1 \right] - I_L + \frac{V - IR_s}{R_{sh}} \quad (4)$$

Where, I_L is the light generated current, I_0 is the dark saturation current, R_s is the series resistance, R_{sh} is the shunt resistance, A is the modified cell or module ideality factor that can be expressed as:

$$A \equiv \frac{N_s n_i K T}{q_e} \quad (5)$$

where N_s is the number of cells or modules that are connected in series, n_i is the diode ideality factor for a cell, K is the Boltzmann constant, q_e is the electron charge, T is the cell or module temperature.

Figure 5 shows the current-voltage (I-V) characteristic curves of a solar cell or a module. Particularly, the power generated by the solar cell or module is the product of the current (I_{mp}) and voltage (V_{mp}). It should be noted that five parameters, such as I_L , I_0 , R_s , R_{sh} , and A , determine the current and voltage generated in a cell or module, thus the impact of external factors, such as solar radiation and temperature could be analyzed from the change of these values. In general, the FF is directly affected by series resistance, and it is found that the fill factor of a solar cell decreases by about 2.5% for each 0.1Ω increase in series resistance [17]. On the

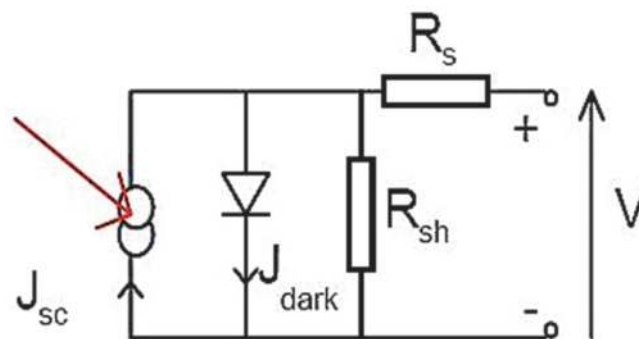


Figure 4. Equivalent circuits for a solar cell in a single diode model, including series and shunt resistance [16].

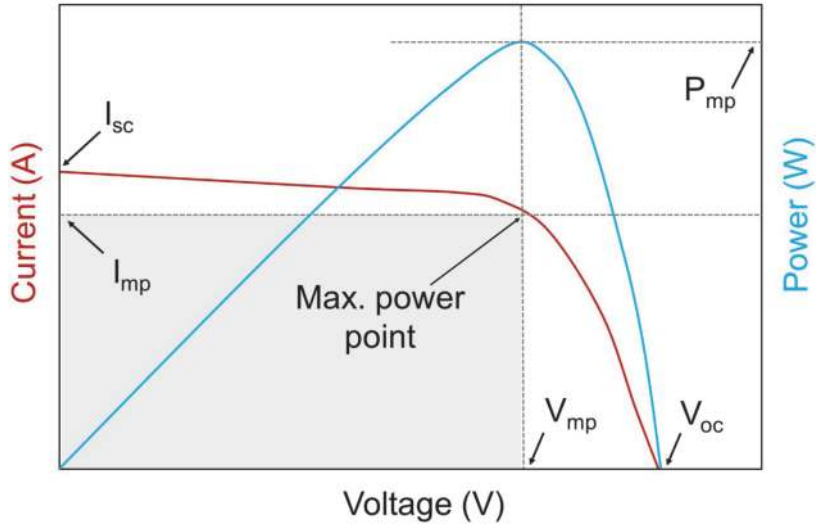


Figure 5.
 Typical current–voltage (I - V) and power–voltage characteristic curves of a solar cell.

other hand, R_{sh} is reduced if the leakage current is increased in a solar cell. If there are any light and temperature-activated defects available in a solar cell, then leakage current could be increased, alternatively R_{sh} could be reduced as the increase of irradiance intensity or temperature. Finally, FF and V_{oc} will be reduced. For an ideal case, $R_s = 0$, $R_{sh} = \infty$ and $n_i = 1$, the open-circuit voltage, V_{oc} could be expressed as,

$$V_{oc} \approx \frac{KT}{q_e} \ln \left(\frac{I_L + I_o}{I_o} \right) \quad (6)$$

For a very small applied voltage ($V \approx 0$), the diode current, I_o is negligible or zero, then from Eq. (6), we can find,

$$I \approx I_L \approx I_{sc} \quad (7)$$

Where I_{sc} is a short circuit current. Now Eq. (9) becomes,

$$V_{oc} \approx \frac{KT}{q_e} \ln \left(\frac{I_{sc} + I_o}{I_o} \right) \quad (8)$$

The V_{oc} and I_{sc} rectangle description as shown in **Figure 5** offers a useful means for characterizing the maximum power point [18]. The fill factor (FF) is defined as the ratio of the maximum power to the product of V_{oc} and I_{sc} and is less than one at all times. FF indicates the squareness of the I - V curves and can be defined from the ratios of two rectangles (**Figure 5**) as,

$$FF = \frac{P_{mp}}{I_{sc} V_{oc}} = \frac{I_{mp} V_{mp}}{I_{sc} V_{oc}} \quad (9)$$

Where P_{mp} denotes the maximum power of the solar cell or module, I_{mp} and V_{mp} are the current and the voltage values at the maximum power point, respectively. Moreover, the most significant Figure of merit for a solar cell or PV module is its power conversion efficiency, η , which is specified as,

$$\eta = \frac{V_{OC} I_{SC}}{P_{in}} FF \quad (10)$$

Where P_{in} denoted the power of incident light that is determined by the characteristics of the light spectrum incident onto the solar cell or PV module. The power of the incident light spectrum, P_{in} can be express as,

$$P_{in} = G \times A \quad (11)$$

Where A is the surface area of the solar cell or PV module and G is the total spectral irradiance, which could be defined as [19],

$$G = \int_0^{\infty} \epsilon_{\lambda} f(\lambda) d\lambda \quad (12)$$

Where, $f(\lambda)$ is the flux density (number of incident photon per unit area and unit time) for a specific wavelength of the photon with energy, ϵ_{λ} and wavelength, λ .

3.2 Spectral response and quantum efficiency

Particularly, the light to the electrical power conversion efficiency of a solar cell or a module is an inherent property that depends on the type of semiconductor material and the manufacturing process. However, this efficiency also depends on the environment of the installation site, especially on the hours of equivalent peak spectral irradiance in a day and/or temperature. The PV module characteristics that we find in the nameplate are typically measured at standard testing conditions (STC), the irradiance of 1000 W m^{-2} at AM 1.5 and $25 \text{ }^{\circ}\text{C}$ of cell temperature. In fact, these conditions hardly exist because the outdoor spectrum is far different from the STC condition, which also varied by location and season. The response to the spectral variation by different types of PV modules vastly depends on its material properties and structure. This response is primarily determined by the bandgap of the materials used in fabrication, which sets the upper wavelength limit of the spectral response (SR). More specifically, SR is depending on the PV material's bandgap, cell thickness, and carrier transport mechanisms in the device. Secondly, device structure, means the position of the absorber material and other supporting layers has a significant effect on the spectral response. Also, the variation of electrical parameters of different types of PV module/device as an impact of various environmental factors depends on the technology (device structure and materials). On the whole, the PV device performance and SR is proportional for specific PV devices, where SR is defined as:

$$SR(\lambda) = J_L(\lambda)/G(\lambda) \quad (13)$$

Where $J_L(\lambda)$ represents the light-generated current density for a specific wavelength " λ " and $G(\lambda)$ is the spectral irradiance of the incident light measured in $\text{W/m}^2\text{-nm}$. However, in state-of-the-art solar cell or PV modules, the spectral response is defined as the short-circuit current, $I_{SC}(\lambda)$, resulting from a single wavelength of light normalized by the maximum possible current [20–23].

$$SR(\lambda) = \frac{I_{SC}(\lambda)}{qAf(\lambda)} \quad (14)$$

Where, q is the electronic charge 1.6×10^{-19} C, A is the surface area of the PV device and $f(\lambda)$ is the incident photon flux (number of photons incident per unit area per second per wavelength). Besides, the SR of the PV devices is also estimated in terms of quantum efficiency (QE), which indicates that how efficiently a PV device converts the incident light to a charge carrier that flows through the external circuit [24], details on QE has been discussed next section. In that case,

$$SR(\lambda) = QE(\lambda) \frac{q \cdot \lambda}{h \cdot c} \quad (15)$$

In the case of PV modules, J_L is approximately the same in value as the short-circuit current density (J_{sc}) [25]. Thus, with the help of the above equations, J_{sc} can be expressed as,

$$I_{sc}(\lambda) = \frac{q}{h \cdot c} \int SR(\lambda) \cdot G(\lambda) \cdot \lambda \cdot d\lambda \quad (16)$$

It could be seen in Eq. (16) that J_{sc} can be estimated by the SR for PV modules which certainly have prime importance in evaluating PV materials and device characteristics. Particularly, the degree to which the SR and the incident irradiance spectrum varies gives rise to a spectral effect on the device current and efficiency. The SR of different types of the module at AM1.5G spectrum (up to 1300 nm) is shown in **Figure 6** to confirm the response is different for different technologies [10]. As seen in Eq. (16), I_{sc} is affected by the spectrum. Particularly, the spectrum variations are also influenced the other PV output parameters, viz. FF, Voc, and η . To determine the magnitudes of these effects on different technology-based PV devices, various performance review studies were carried out [26–31].

Particularly, The SR shows represent the current produced by a solar cell for per watt of irradiance at each wavelength of the photon. As seen in **Figure 7** that SR towards the higher wavelength region is lower because photons in this region have energy less than the material bandgap threshold. As a result, the effect of spectral variation on the output of PV devices is most pronounced in narrow SR technologies such as a-Si and CdTe. Especially narrowest SR is seen for the a-Si that is also discussed in the literature [32–35]. For simplification of SR and PV performance,

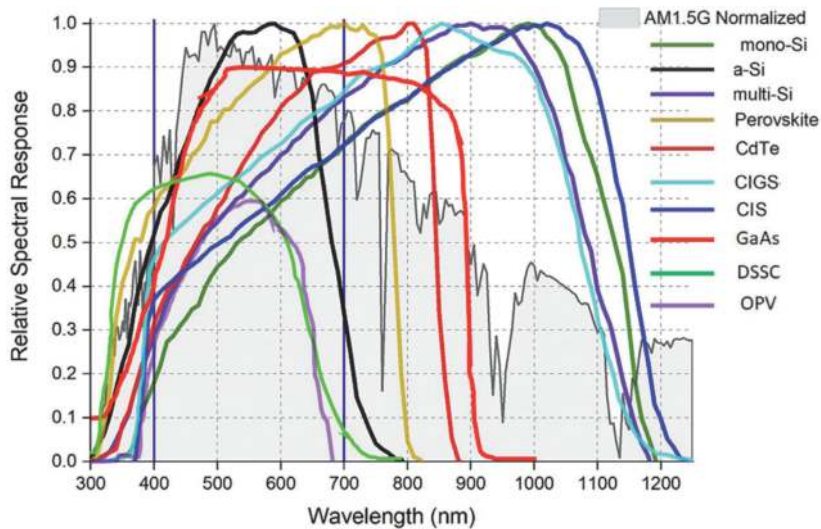


Figure 6. Spectral response characteristics of different solar module technologies, modified from [26–35].

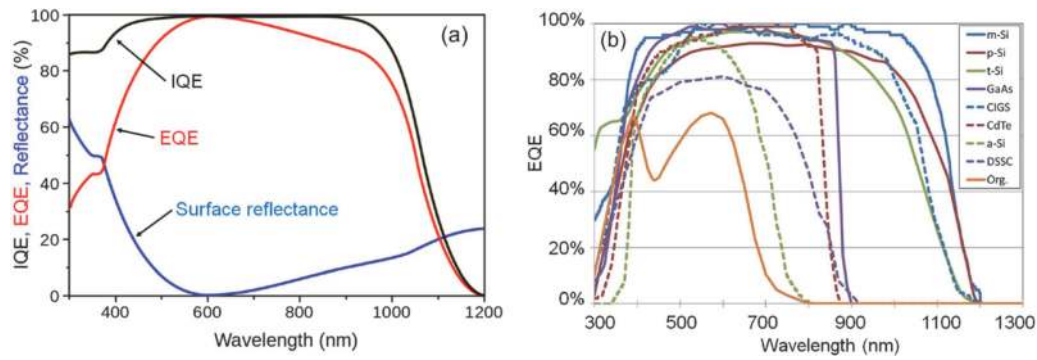


Figure 7. (a) variation of EQE, IQE, and reflectance with the wavelength of a c-Si solar cell (collected and modified from Wikipedia), (b) EQE of different PV solar cell technology [41].

research is commonly used one-dimensional terms, such as spectral mismatch factor (MMF) [32–34, 36], the useful fraction (UF) [37], average photon energy (APE) [38, 39]. In the case of MMF and UF, their values should be a known factor for a specific module under study, however, the SR data is not available publicly and analysis complexity arises. Besides, APE is denoted by the unit of an electron volt (eV) which signifies the average incoming photon energy. The equation for calculating is as follow:

$$APE = \frac{\int_{p\lambda}^{q\lambda} E(\lambda) d\lambda}{q_e \int_{p\lambda}^{q\lambda} f(\lambda) d\lambda} \quad (17)$$

Where, $E(\lambda)$ represents the energy of the incident photon and $f(\lambda)$ is the incident photon flux at wavelength λ , and $p\lambda$ and $q\lambda$ are the integration limits indicate the lower and higher absorption wavelength, which are 300 and 1200 nm as shown in **Figure 7**. Particularly, APE varies on a daily and seasonal basis due to the increase of air mass at sunrise and sunset compared to noon and in winter compared to summer. For example, when the sun is above the horizon, the spectral irradiance is red-shifted and the APE becomes low. APE rises again to a high around noon during the day. Moreover, the APE is higher in the summer months than in winter because the zenith angle of the sun is higher in summer. Besides, the atmospheric water, cloud cover, and/or aerosol content affect the APE due to light absorption and scattering. For most of the PV modules, the APE effect on performance seems to be linear. The spectral photon flux density denoted in joules can be expressed as below for a specific wavelength λ :

$$f(\lambda) = \frac{G(\lambda)}{E_\lambda} = \frac{G(\lambda)}{\frac{hc}{\lambda}} \quad (18)$$

where ‘h’ is the Planck constant and ‘c’ is the light velocity in vacuum.

The SR and QE are conceptually similar to each other. Particularly, SR is the ratio of the generated current in a solar cell per unit incident power, while QE denoted the ratio of the number of generated carriers and the number of the incident photon on the solar cell. In another way, the QE of a solar cell represents the amount of current the cell produces for a particular wavelength of an incident photon. Knowing the QE of a particular PV technology is important because by integrating QE for the whole solar spectrum, the current generation capability of PV solar cells could be realized. Interestingly, the QE value could exceed 100% for a PV solar cell in the case of multiple excitation and generation (MEG). In that case, one incident photon

could generate several electron–hole pairs as an impact of multiple excitations. The MEG properties are typically seen in quantum-dot solar cells [40]. However, all the incident photons on the cell surface cannot be absorbed due to surface optical properties, such as absorption and reflection. Thus, QE is divided into two terms, (i) external QE (EQE) and (ii) internal QE (IQE) which simply differ by the photons reflection properties of a PV solar cell. In the case of EQE, all photons that impinge on the cell surface are taken into account, while in the case of IQE, only photons that are absorbed (not reflected) by the solar cell are considered. The graphical representation of EQE and IQE is shown in **Figure 7**.

High EQE is a precondition for high-power PV applications, which depends on the absorption coefficient of the absorber material of a PV solar cell, the carrier excitation quality, and carrier recombination rate or the amount of electron transport to the electrodes. The mentioned QE in Eq. (15) is typically EQE, which is directly related to the current generation by a solar cell [41]:

$$J_{sc} = q \int_0^{\infty} \phi_{\lambda}(\lambda) \cdot EQE(\lambda) \cdot d\lambda \quad (19)$$

Where, with q is the charge of electron and $\phi_{\lambda}(\lambda)$ the incident spectral flux density, indicating the incident number of photons of wavelength λ on the cell surface per unit of area, per unit of time and EQE could be defined as:

$$EQE = \frac{\text{electron/s}}{\text{photon/s}} = \frac{\text{current/e}}{\text{total photon power}/h\nu} \quad (20)$$

The relation between IQE and EQE could be defined as:

$$IQE = \frac{EQE}{1 - L} = \frac{EQE}{1 - R - T} \quad (21)$$

Where L is the total optical loss that occurred in a solar cell either through reflection or transmission or both. Particularly, for maximizing EQE, the optical loss should be minimized. To reduce the optical loss, anti-reflection coating, and back-reflection coating is applied in the current PV technologies.

3.3 Spectral irradiance and temperature

Solar irradiance and surface air temperature are two key factors for investigating the PV module performance. Particularly, the increase in solar irradiation is a cause of the increase in air temperature and vice versa. On the other hand, the increase in solar irradiance is proportionally increased the power output of the PV module, however, module output decrease with the increase of temperature [42]. Usually, the output and temperature of the PV modules are considered to be linear. The effect of temperature mostly depends on the absorber material and its quality. From the module electrical properties, the temperature effect could be realized by observing the variation of the device parameters:

$$P_{mpp} = I_{sc} V_{oc} FF \quad (22)$$

In the case of I_{sc} and FF , there is very little change that occurred with temperature for crystalline silicon and thin-film devices. Alternatively, the V_{oc} is highly dependent on the temperature variation, which can be described via the V_{oc} as calculated from the one diode model as shown below:

$$\frac{d}{dt} V_{oc} = \frac{d}{dt} \left(n V_T \ln \frac{I_{sc}}{I_0} \right) \quad (23)$$

And,

$$V_T = \frac{kT}{q} \quad (24)$$

Where V_T is known as thermal voltage, T is the solar cell temperature, k is the Boltzmann constant, q is the elemental charge q , n is the ideality factor and I_0 is the diode saturation current. From the above diode equation, it could seem that the V_{oc} is positively changing with the temperature, because the above-simplified diode equation typically overlooked the parasitic factors, such as solar cell series and shunt resistance. Particularly, this parasitic resistance is changed significantly over thermal variation [43] and greatly impacts the voltage and diode saturation current as reported elsewhere [44]. For understanding the impact of temperature on V_{oc} , we have to consider the temperature-dependent diode saturation current, which in turn:

$$I_0 = B T^\gamma \exp \left(\frac{E_g}{kT} \right) \quad (25)$$

Where B is a temperature-independent empirical factor but controlled by the quality of absorber material, γ is also an empirical factor that relies on the specific carrier loss mechanism and E_g is the absorber material bandgap. The influence of irradiance and module temperature can be explored by combining the data according to these dependencies. The resulting matrix can then be used to model the annual yield for various technologies at different locations [45]. The main uncertainties, in this case, are kWp standardization and input irradiance [46].

3.4 Solar spectrum distribution model

As there are several uncertainty factors are involving, for the easy and efficient deployment of PV solar cell system, it is essential to measure and develop a model for the spectral distribution of solar radiation. Colle et al. [47] have shown that there has a linear relationship between the uncertainty of solar irradiation and the uncertainty of solar thermal and PV systems. This is a big challenge in the 21st century to develop a more efficient and robust model that could reduce the solar radiation misprint include will need fewer input parameters, will have smaller residual and can be used in a wide variety of conditions.

Indeed, the solar spectrum depends on the place, time, and condition of the atmosphere. The global solar spectrum may be divided into two spectrum models, one for direct beam radiation and the other for diffuse radiation. Particularly, the spectrum of solar incident radiation wavelengths on the PV modules corresponds to the appropriate spectral response range of the PV cells. Several reports on the effect of spectral irradiance variation and PV solar cell performance can be found elsewhere [48, 49]. The longer irradiation hours provided the better annual average electricity outputs [50]. The effect of solar spectral irradiation on the yield of several PV technologies has been documented by Nann and Emery at four separate locations [51]. Eke et al., on the other hand, found that the spectrum variance had a very limited effect on the low bandgap absorber content in PV solar cells [52]. **Figures 6** and **7** shows the spectral response characteristics and EQE of different PV technologies which indicate that how the performance of PV module could change upon the variation spectral distribution.

Several solar spectrum models, including SPECTRAL2 [53], LOWTRAN2 [54], REST2 [55], and SMARTS2 [56], have been developed yet to date over time for clear skies. These models are usually computer programs developed to evaluate the shortwave spectrum components of surface solar irradiance in the range of 280 to 4000 nm. Some of them have high spectral resolutions, however, they need very complex calculations making them less efficient. In the case of LOWTRAN(2), detailed inputs are needed, which increases the execution time and creates some performance limitations, that's why the use of this model is limited in engineering applications [57]. On the other hand, even a low number of parameters are needed for SPECTRAL2, however, the mean deviation associated with different aerosol models is higher than SMART2 [58]. On the other hand, transmittance parameterizations based on the SMARTS spectral model are used to build the high-performance REST2 model [57]. Particularly, more updated parametric functions and constants are used in the SMARTS2 model, for which it has a higher resolution and is showing lower deviation in the spectral analysis. SMARTS program is written in FORTRAN and depends on simplifications of the radiative transfer equation which allow very quick calculations of the irradiance of the surface. The newest versions, such as SMARTS2.9.2 and SMARTS 2.9.5 are hosted by NREL.

The SMART model uses different inputs to define the conditions of the atmosphere under which the irradiance spectra are to be measured. Ideal conditions can also be selected by the user, based on various potential model atmospheres and aerosol models. Moreover, it is also possible to determine practical conditions as inputs, based, for example, on aerosol and water vapor data supplied by a sun photometer [59]. Besides, the spectrally integrated (or 'broadband') irradiance values are given by this model, which can later be compared with measurements from a pyranometer (for diffuse or global radiation) or pyrheliumeter (for direct radiation). Solar geometry is another vital input in this model in addition to the atmospheric condition, which is typically specified by the position of the sun (zenith angle and azimuth), the location, the air mass (AM), or by specific time and date. More details on the usage of the

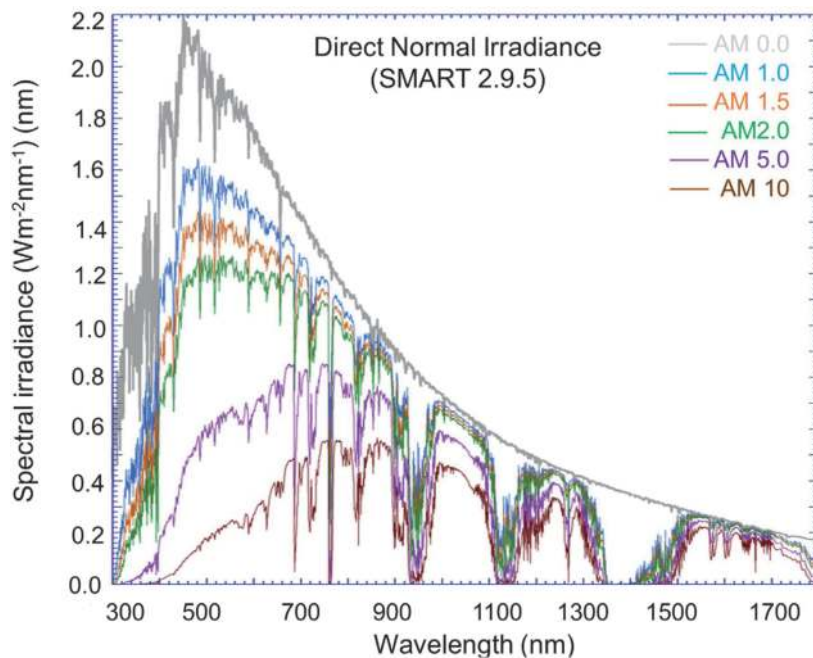


Figure 8.

Direct normal irradiance spectra calculated with SMARTS 2.9.5 for increasing air mass (0 to 10), using the same atmospheric conditions as the ASTM G173 standard. Air mass 0 corresponds to the extraterrestrial spectrum, marked as top of atmosphere (TOA), modified from [67].

SMARTS model for PV applications can be found elsewhere [60–63]. Particularly, this model is frequently employed to evaluate PV modules' efficiency and mismatch factors in real-world conditions [64–66]. **Figure 8** shows the direct normal irradiance spectra with SMART 2.9.5 for different air mass.

4. Performance of PV modules by technologies

Crystalline silicon (c-Si) is the most prevalent PV technology on the market (c-Si). In considering crystal size and crystallinity, c-Si can be divided into two major categories, mono or single-crystalline Si (sc-S) and multi or polycrystalline Si (mc-Si). The power conversion efficiency of sc-Si is higher than mc-Si solar cells, alternatively, sc-Si is costly than mc-Si. The typical efficiency of commercial c-Si modules is between 11% and 20% which power generation varies by temperature (temperature coefficients) in the range of 0.3–0.5%/K [68]. Commercial c-Si modules consisting of 200–500 μm thick PV cells that are connected in series and/or parallel for attaining expected voltage and current. It is important to note that c-Si solar cells or PV modules can generate electrical energy for a wide range of the spectrum (350–1200 nm) as illustrated in **Figure 9** [69]. However, the absorption coefficient of c-Si is below 10^4 cm^{-1} for all wavelengths larger than 500 nm as shown in **Figure 9**. This means that all the potential photons below 500 nm are absorbed close to the surface of the cell. Thus, it is important for the c-Si solar cell that the active region has to be located near the cell surface for absorbing all potential photons and achieving optimum efficiency. Also, it could be seen in **Figure 9** that the absorption coefficient is below 2.0×10^4 for wavelength above 650 nm. As the absorption coefficient of c-Si is below 10^3 for wavelengths above 700 nm which indicates that photons in this range can penetrate the bulk and generate electron–hole pairs. However, their contribution to the photocurrent is very hard in the case of conventional c-Si solar cells. Thus, for collecting these bulk carriers, the configuration of conventional c-Si structure modified, by names they

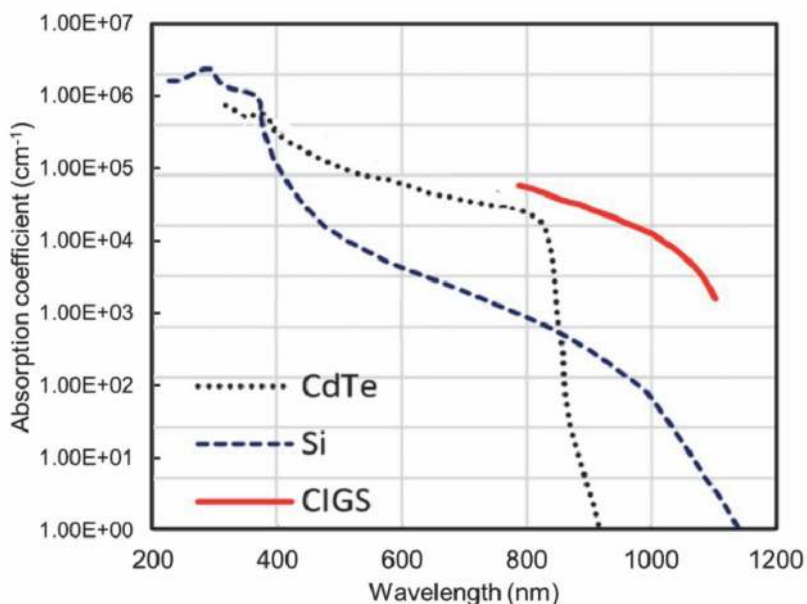


Figure 9. Absorption spectrum of Si, CdTe, and CIGS solar cells, modified from [69].

are passivated emitter and rear contact (PERC) [70], passivated emitter and rear locally-diffused PERL [71], interdigitated back-contact (IBC) c-Si [72] solar cells.

As it has been mentioned earlier that the response to spectral variation by different types of PV modules vastly depends on its material properties and structure, c-Si solar cells also showed different characteristics depending on the irradiation properties. Several studies have been reported on the in-field energy output analysis of c-Si PV systems by Panchula et al. [73] based in Ontario, Canada; Dolara et al. [74] based in Tuscany, Italy; Fiances et al. [75] Based on a different place in Peru, Kazem et al. [76] based on the desert area of Sohar, Oman, Fuentes et al. [77] and Muñoz et al. [78] under warm climate of Spain, Bahaidarah et al. [79] based on Dhahran, Saudi Arabia and Edalati et al. [80] based on Kerman, Iran. In the above reports, they typically estimate the performance of the system based only on average monthly or yearly insolation and performance ratio varied by the location ranging from around 0.7 to 0.85. Fiances et al. [75] studied different Si technology includes sc-Si, mc-Si, a-Si, and μ c-Si PV modules in the climate of Peru, and finalize that a-Si/ μ c-Si PV modules perform much better than others with an annual performance ratio of 0.97. Ahmed Ghitas [81] reported the effects of the spectral variations on the mc-Si module performance based on outdoor measurements in daily irradiation changes. They only consider cloud-free days in Helwan, Egypt in their measurements and also did not consider the temperature effect. The variation of V_{oc} , J_{sc} , and power concerning radiation intensity is shown in **Figure 10**. It is evident from **Figure 10** that the most affected device parameter is J_{sc} , and output power in the case of the mc-Si PV module.

Eke and Demircan [82] have been studied mc-Si PV module performance based on winter (January) and Summer (August) for Mugla, Turkey. The operating temperature at this location is 50.5 °C in January and 80.5 °C on August 16. The power generation of the module is 30% lesser in summer than winter because of the significant difference in operating temperature. The power generation every day in January and August is shown in **Figure 11**. Bora et al. [83] also studied the pc-Si PV module along with a-Si, HIT-Si PV modules under the climate condition of the different parts of India. They find that all these three types of Si-based PV modules produce the highest energy yield in the cold and sunny zone.

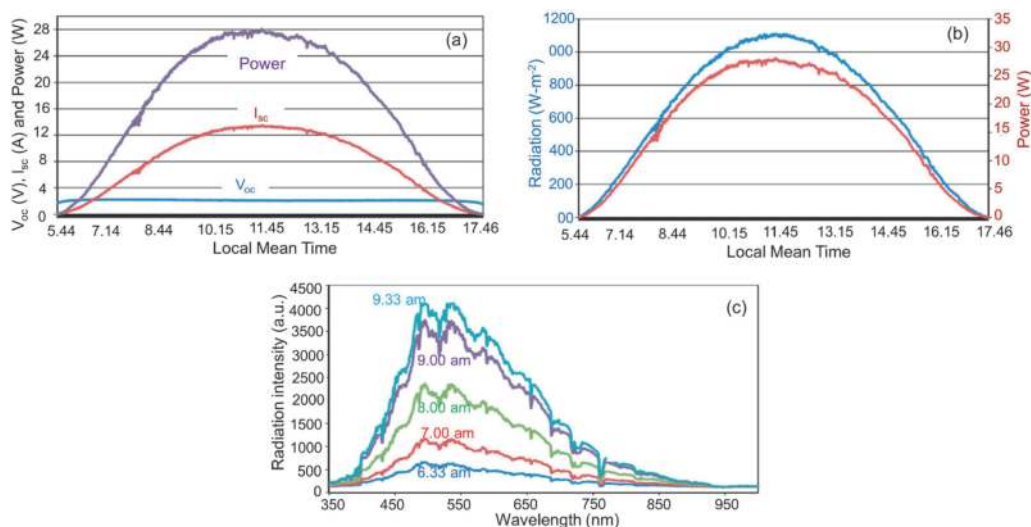


Figure 10.

(a) Daily profile of the measured solar module short circuit current, open-circuit voltage, and electrical output power, (b) daily profile of incident solar radiation along with module output power, and (c) spectral irradiance variation versus time (a.ms) on a clear sky measurement day [81].

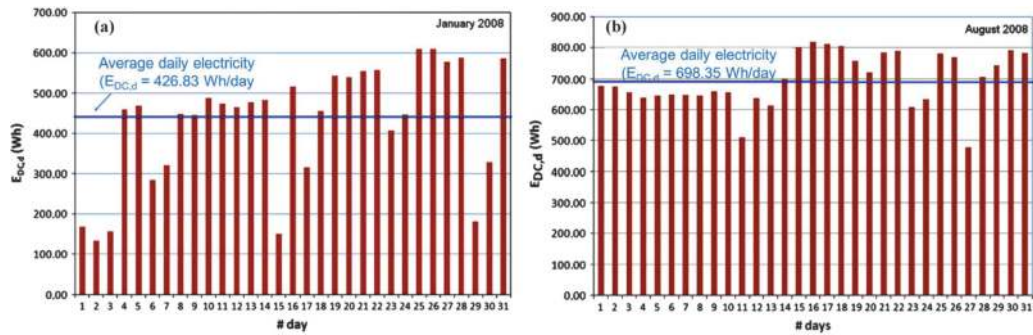


Figure 11. PV module performance in January (a) and August (b) 2008 for Mugla, Turkey environment [82].

It is important to mention that the energy yield analysis of a PV system is incomplete if their low light condition analysis is missing. Reich et al. [84] have reported the performance of c-Si at low light conditions, however, the impact of temperature is missing as they conducted the study focusing on indoor performance. The finalized that the obtained efficiency via indoor measurement and rated efficiency has a significant difference. Certainly, temperature is a dominant factor in the performance of the PV system in outdoor conditions. It should be noted that solar irradiance and ambient temperature are proportional. Chander et al. [85], and Atsu and Dhaundiya [86] studied output yield using a detailed model that includes temperature and wind speed variation. Chander et al. [85] reported that the performance parameters of the sc-Si module such as Voc, Pmax, FF, and efficiency are decreased with temperature while the Jsc is increased. Bahaidarah et al. [73] also suggested that for achieving the highest PV performance yield in Saudi Arabia, a suitable and uniform cooling system is necessary due to the climatic conditions. A detailed study on performance variation by low light conditions along with the temperature variation effect has been presented by Pervaiz and Khan [87]. In their

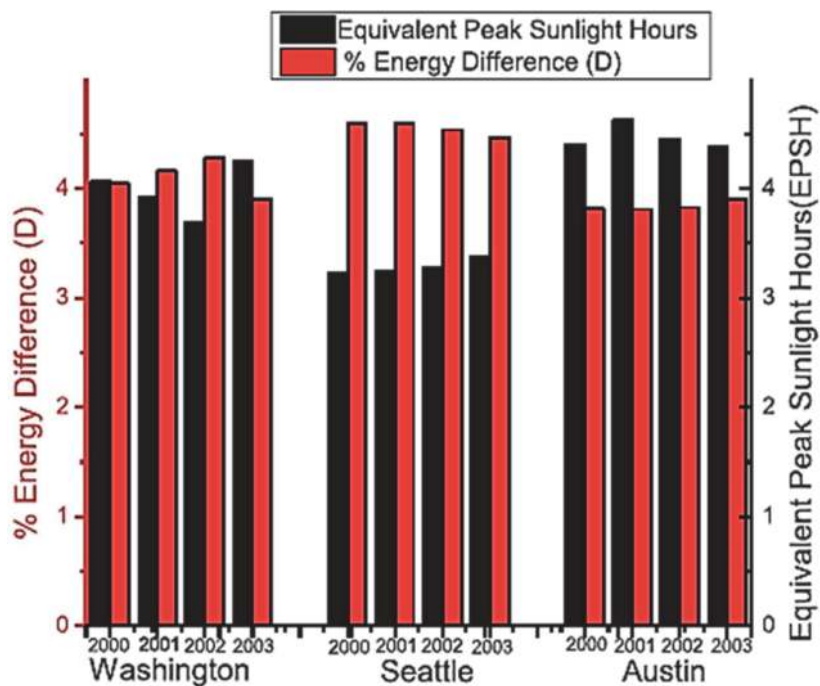


Figure 12. Energy difference (D) in percent for Washington, Seattle, and Austin for years 2000–2003 [78].

modeling, they used various insulation profiles for a different location in the US collected from NREL. They reported that the energy harvesting of a PV system for a specific location depends on the average peak sunlight hours of that location as shown in **Figure 12**. The use of the following equation for calculating energy difference concerning the variation of Equivalent Peak Sunlight Hours (EPSH).

$$\text{Energy difference, } D = [(E_i - E_c)/E_i] \times 100 \quad (26)$$

Where E_i is the energy harvested during one year considering a constant efficiency and E_c is the energy harvested incorporating a change in efficiency. They finalized that the reduction in energy yield is reliant on the EPSH of a region where reduction factor could range from 1.5 to 5% for various regions concerning the value of the EPSH.

Cotfas and Cotfas [88] have been studied details on the performance of sc-Si and a-Si PV modules under the natural condition via years of observation, in Brasov, Romania. They reported that the average P_{max} of the sc-Si module is two times greater than the a-Si module, however, on clear winter days, the values even increase near to three times greater. Also, at low irradiance, under 100 W/m^2 , the power gain is of sc-Si is 1.9 times greater than a-Si. The gain is over 1.9 times even for very low irradiance, under 100 W/m^2 . The detailed performance of the a-Si PV module including other thin-film modules as an impact of irradiance and temperature are covered in the next section. Under the Mediterranean climatic conditions of the north of Athens, Greece [89], the performance of the p-Si photovoltaic system has been investigated. There is a linear relationship between the module surface temperature and the irradiance where the average temperature about $49.9 \text{ }^\circ\text{C}$ in summer and $16.8 \text{ }^\circ\text{C}$ in winter. The efficiency of the p-Si module has been significantly dropped in summer where it ranging from 6.2% to 10.4% concerning the module temperature.

The SR of PV cells depends on the absorption coefficient and/or bandgap of the absorber materials. Similarly, the performance variation by increase or decrease of temperature also depends on the bandgap [90]. The semiconductor material with a wider bandgap, such as 1.04–1.68 eV for CIGS [91], 1.45–1.5 eV for CdTe [92, 93], and (1.7–1.9 eV for a-Si [94] shows higher temperature resistance to the increase of

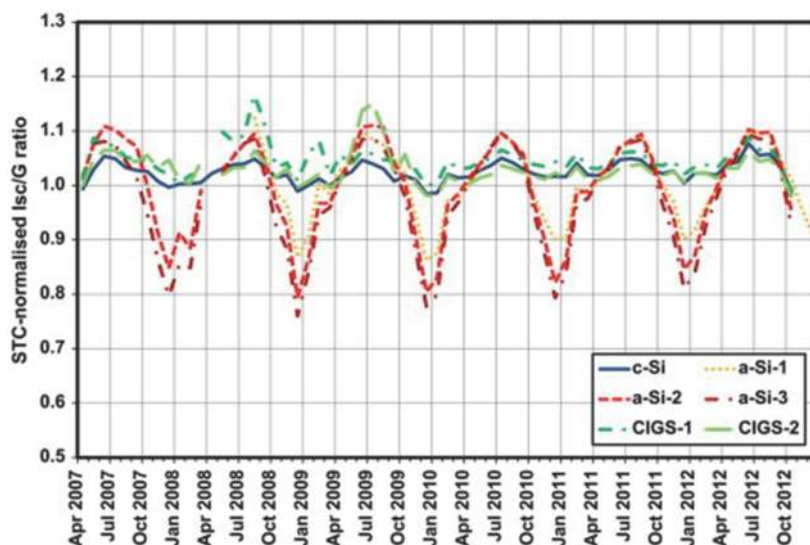


Figure 13.

Calculated spectral effects for the devices under test in the UK environment. The graph compares the normalized ISC divided by the irradiance measured with the pyrometer [86].

module temperature. As a consequence, they have a lower temperature coefficient than sc-Si and pc-Si PV modules [95], and thus, device performance is significantly affected by the temperature. The details on the effects of irradiance, spectrum, and temperature on thin-film PV modules were investigated by Gottschalk et al. [96] under the UK environment. It has been reported that the performance of a-Si is highly spectral dependent as shown in **Figure 13**. The relative change in short circuit current (I_{sc}) is +10% to –20% observed for a-Si whereas the change is only $\pm 3\%$ for c-Si and CIGS. Environmental effects have also been shown to cause up to 15% of losses to the annual PV production. The spectral impact on different PV technologies for all single months has been investigated under the German climate condition [32]. Similar to the other reports, the spectral impact changes more for bigger bandgap a-Si PV modules as shown in **Table 1**. The average gains over the year are 3.4% for a-Si, 1.1% for c-Si, 0.6% for CIGS, and 2.4% for CdTe. It has been reported that CIGS and c-Si modules exhibit high gains in winter and a-Si and CdTe shows an advantage in summer attributed mostly to spectrum variation [32]. The study carried in the Netherlands [97] showed that low irradiance caused a decrease in annual energy yield of 1.2% for the CIGS modules and 1% for CdTe. This experimental study also indicated a strong effect of spectral variation on the performance of the a-Si modules.

The detail on performance variation by the influence of temperature of the different types of PV modules has been conducted by Gutkowski et al. under the low insolation climate of Poland [95]. They observed a significant difference in performance by different PV modules at temperatures 15–48 °C as shown in **Figure 14(a)**. It is clear from **Figure 14(a)** that under real conditions of the high-temperature region, the power generated by CIGS thin-film technologies is higher compare to the pc-Si PV modules. Ozden et al. [98] also experimentally investigate the a-Si and CdTe thin-film PV module performance under the Turkey climate zone along with sc-Si and mc-Si. They found a significant difference in performance in that module for the sunny and cloudy days as shown in **Figure 14(b)**. The output performance of sc-Si and mc-Si is found to be the same, but the output difference

<i>i</i>	Gi [kWh] average monthly irradiation from the reference period	Average, relative monthly spectral impact				
		a-Si (%)	CdTe (%)	c-Si (%)	High-eff. c-Si (%)	CIGS (%)
1	38	–2.0	1	1.9	2.4	2.6
2	65	–1.3	0.1	1	1.4	1.6
3	122	0.1	0.6	0.7	0.8	0.9
4	141	3.5	1.9	1.2	0.9	0.4
5	166	4.2	2.3	1.5	0.9	0.3
6	166	5.1	2.8	1.4	0.8	0
7	184	5.3	3.4	1.5	0.8	0
8	168	5.3	3.5	1.6	0.9	0.1
9	136	4.3	3.1	1.5	1	0.4
10	91	2.8	3	1.9	1.7	1.3
11	43	0.8	2.3	2.1	2.2	2.1
12	35	–2.2	1.8	2.4	3	3.3

Table 1. Calculation of annual spectral impact based on the monthly sums of irradiance of a reference year and the determined average monthly spectral impact assessed in Germany [32].

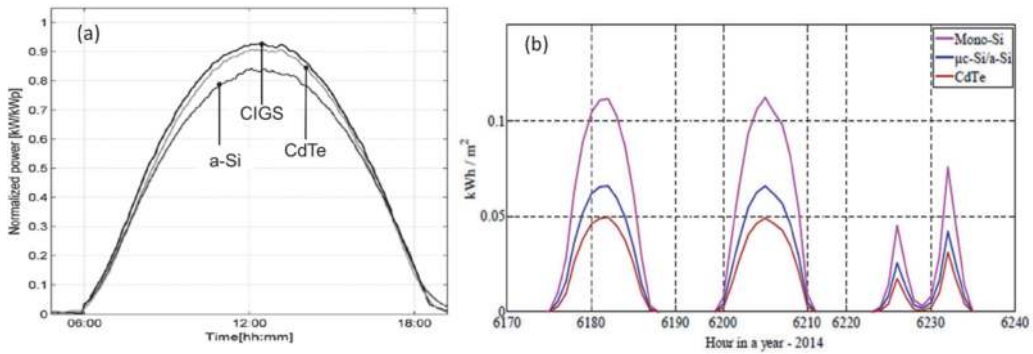


Figure 14. (a) Normalized DC power generated by the PV systems of each studied technology [95], and (b) maximum irradiance and temperature recorded for that day were 1000 W/m² and 55 °C [78].

between CdTe and sc-Si modules is 60% for a sunny day and which reduces to 35% for a cloudy day indicating the impact of irradiance as well as temperature on these technologies. Moreover, the performance ratio (PR) of sc-Si is in the range of 70%–90%, a-Si is about 70% and CdTe is only 42%–72%. Alternatively, Kesler et al. [99] also conducted a performance analysis between the c-Si and thin film for another location, Antalya, Turkey, and reported that performance of the both technology is very close to each other. Even they specified the reason is the high ambient temperature of that area, however, the rated efficiency of that technologies may play an important role in this case, which means that if the rated efficiency is almost the same, their performance will be close to each other.

Sharma et al. [100] studied three different PV technologies, such as a-Si, pc-Si, and HIT under the tropical climate of India. They found that the best-suited PV technology for this climate is HIT and a-Si. The overall performance ratio for a-Si is 90% and for pc-Si is 83% in this region as shown in **Figure 15**. Interestingly, the energy yield of a-Si is 14% greater during summer, but 6% lower in winter. The effect of seasonal which in turn the effect of irradiance and temperature on the performance of a-Si may be related to its thermal annealing process [101]. The HIT modules have consistently performed better (≥ 4 –12%) than p-Si over the year.

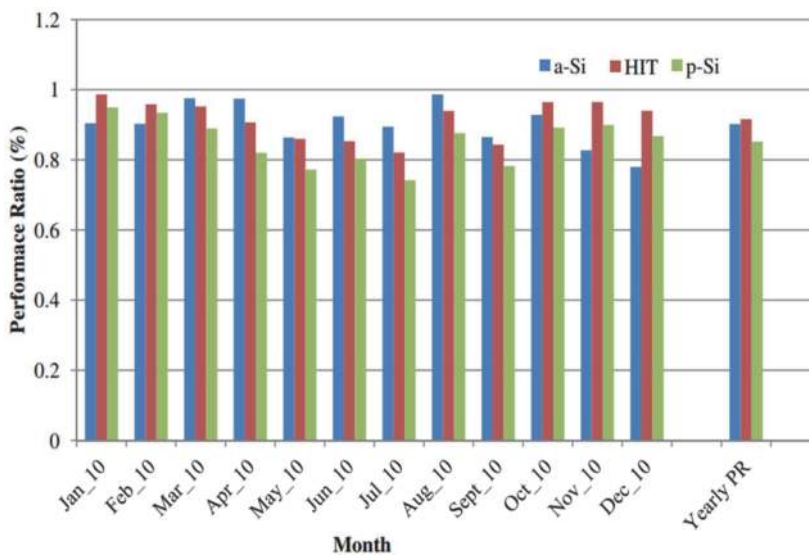


Figure 15. Comparison of measured monthly and yearly performance ratio of each technology array tested in Indian climate condition [100].

Aste et al. [102] investigate PV module performance under temperate climatic conditions (Italy) where the more distinct seasonal change and/or wide temperature variation have occurred. They found that a-Si is much more sensitive to the seasonal solar spectrum rather than c-Si and HIT technology. The highest 93% of performance ratio has been reported for c-Si in this study. However, the c-Si technology has also shown seasonal variation as an exceptional case [75] and the performance ratio found 20% lower in summer than in winter as a role of temperature variation. In summer, the a-Si/mc-Si stack cell showed higher performance than the other technologies tested in this study, which may be due to its low-temperature coefficient and thermal annealing.

The assessment carried in the Netherlands [103] showed that the CIGS modules are strongly affected by irradiance and temperature variations with a decrease in annual energy yield of 1.2%. Moreover, CdTe modules also exhibited a decrease in energy yield of about 1.0%. This experimental study also showed a significant influence of spectral variation on the efficiency of a-Si modules. Zdyb and Gutkowski studied four different types of PV modules, such as pc-Si, a-Si, CIGS, and CdTe at high latitude under East Poland climate conditions [104]. In their study, a-Si and CIGS shows the gain in performance ratio (about to 73.4% for a-Si and 90.7% for CIGS) during summer sunny and warm environment. The increase of performance ratio of a-Si PV modules has also been reported by Makrides et al. [101] studied under the Cyprus environment. On the other hand, the performance ratio of pc-Si PV modules exhibited over 80% except for December and always remain the highest among the investigated PV modules over the year as shown in **Figure 16**.

The effect of spectral irradiance distribution on the performance of a-Si/mc-Si stacked photovoltaic modules has been analyzed by Minemoto et al. [105] installed at Kusatsu-city (Japan). Their study revealed that these stacked PV modules are extremely spectrally sensitive compared to pc-Si PV modules installed on the same site. Akhmad et al. [106] have been compared the performance of poly-silicon (pc-Si) and amorphous silicon (a-Si) at Kobe, Japan, and found a-Si modules are better for this region. K. Nishioka et al. [107] compared sc-Si, pc-Si module, and heterojunction silicon at Nara Institute of Science and Technology (NAIST) under Japanese climate. They reported that the HIT technology is better suited for this region due to its low-temperature dependency. Poissant [108] has evaluated four

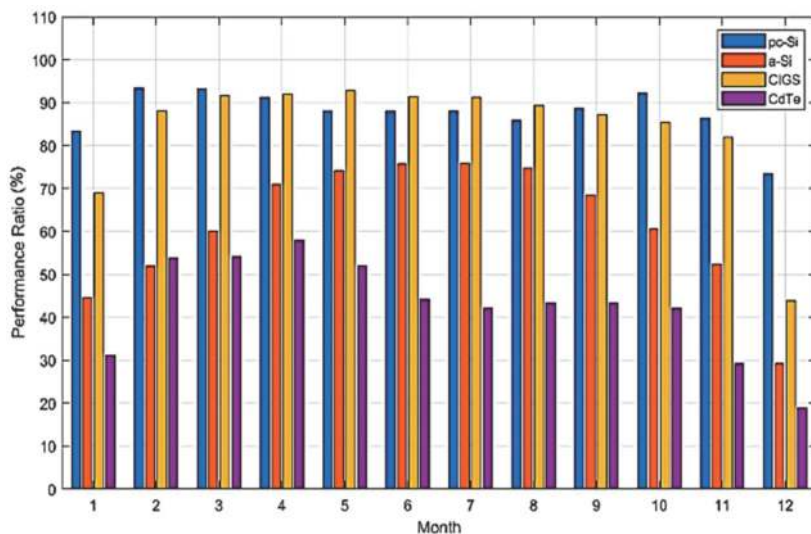


Figure 16. Performance ratio for each studied PV technology investigated in East Poland (data collected in 2018) [104].

different novel PV module technologies, (i) H-Si, (ii) IBC, (iii) a-Si/uc-Si, and (iv) c-Si under the climate of Canada. His study confirmed that the heterojunction silicon and a-Si/uc-Si technologies are less affected by temperature than the other two crystalline silicon technologies. Canete et al. [109] also performed a comparative study of four different photovoltaic module technologies, (i) amorphous silicon (a-Si), (ii) tandem structure of amorphous silicon- microcrystalline silicon (a-Si/-mc-Si), (iii) polycrystalline silicon module (pc-Si) and (iv) cadmium telluride (CdTe). Their results show that the performance of thin-film modules is better than that of pc-Si modules for the location of Southern Spain. The performances of c-Si

Author(s)	Location	Environmental Parameters	Tested Technologies	Best Perform Technology
Dirnberger et al., 2015 [32]	Breisgau, Germany	Maritime climate, 5-25 °C, 1,117 kW/m ² /year (approx.)	a-Si, sc-Si, CIGS and CdTe	a-Si
Francis et al., 2019 [75]	i. Arequipa, Peru Tacna, Peru Lima, Peru	i. Diverse climates 2380 kW/m ² , 3.81-32 °C 2280 kW/m ² , 13.4-31.5 °C 1740 kW/m ² , 18.8-18.9 °C	i. sc-Si ps-Si a-Si/uc-Si	a-Si/μc-Si
Edalati et al., 2015 [81]	Kerman, Iran	Dry climate 68.64-198.72 kW/m ² , 20 °C	sc-Si, and pc-Si	pc-Si
Bora et al., 2018 [83]	Different parts of India	0.82-0.87 kW/m ² /day not mentioned	a-Si, HIT, and pc-Si	All (cold and sunny zone)
Cotfas and Cotfas, 2019 [88]	Brasov, Romania	Temperate-continental climate, 2.1-1.82 Wh/m ² /day, -4.0 - 24 °C	sc-Si and a-Si	sc-Si
Louwen et al., 2016 [89]	Utrecht, Netherlands	Oceanic climate, 20.5-29.5 °C, 950-1050 W/m ²	SHJ, a-Si, sc-Si, pc-Si, CIGS, CIS and CdTe	sc-Si and SHJ
Gulkowski et al., 2019 [95]	Lublin, Poland	Temperate climate, 950-1250 (kWh/m ²)/year, 15-48 °C	CdTe, CIGS, and pc-Si	CIGS
Aste et al., 2014 [94]	Milan, Italy	Temperate climatic, 1270 kW/m ² /year, -5-32 °C	c-Si, a-Si/uc-Si, HIT	HIT
Zdyb and Gulkowski, 2020 [103]	Lublin, Poland	Temperate climate, 950-1250 (kWh/m ²)/year, 15-48 °C	pc-Si, a-Si, CIGS, and CdTe	pc-Si and CIGS
Makrides et al., 2018 [104]	Cyprus	Mediterranean climate, 1988-2054 kWh/m ² , 10-40 °C	sc-Si, pc-Si, a-Si, CIGS and CdTe	a-Si
Minemoto et al., 2007 [105]	Kusatsu-city, Japan	Subtropical climate, 200 kW/m ² , 9-33 °C	pc-Si, and a-Si	pc-Si
Poissant, 2009 [108]	Montreal, Canada	Continental climate, 950-1050 W/m ² , max. 20 to 22 °C	SHJ, IBC, a-Si/uc-Si, and c-Si	a-Si/uc-Si
Cañete et al., 2014 [109]	Southern Spain	Dry Mediterranean climate, 3.7-7.4 kWh/m ² /day, 15-30 °C	a-Si, a-Si/μc-Si CdTe, and pc-Si	a-Si and CdTe

Table 2.

Summary of few reported works for finding out the best PV technology by location and climate.

and a-Si PV modules under South Africa climate conditions have been evaluated by Maluta and Sankaran [110]. They found that both technologies give a similar and suitable performance for the climate of this region. Three different PV technologies (monocrystalline, polycrystalline, and amorphous silicon) have been evaluated under the desert climate by M. Shaltout et al. [111]. They reported that the polycrystalline silicon cells are more suitable in such a climate. All these above-mentioned studies indicate the difficulty when it comes to choosing the appropriate PV technology for a given site. Thus, the prediction of PV energy potentials before installation helps us to understand the economic advantages associated with it and for policy regulation for electric utilities.

Table 2 shows the summary of a few reported works for finding out the best PV technology by location and its climate. It should be noticed that the results reported by the various researcher as mentioned above are very difficult to compare because the work has been conducted focusing on different locations and various time scales (instantaneous, monthly, annual), different energy effects, and even the works are different by used metrics and calculation. However, it is well agreed that the impact of spectral irradiance variations on PV device performance mostly depends on its spectral response, which in turn depends on its absorber material properties and quality. Moreover, the influence of spectral irradiance on PV performance is dependent on installation sites, for instance, the spectral distribution, climate, environment, latitude, longitude, albedo, etc. of the location. Besides, the spectral distribution of specific sites again depends on the cloudiness, water-vapor and aerosol content in the sky of that sites. The analysis considering all the above factors certainly will be too difficult, thus, the researcher considers only some of the factors for simplifying their work.

5. Conclusion

The weather and/or solar irradiance of the earth is significantly different from one location to another. Again, solar irradiance varies for a specific location by season and/or common weather phenomenon, such as dust, rain, wind, cloud, fog, and snow, etc. Thus, every year solar irradiance also not the same in amount and as an impact of the above factors, the energy yield of different PV technology is affected differently and prediction is very complicated. However, numerous studies could help us to predict which PV technology is better suited for a certain location. It should be noticed that all the incident solar radiations absorbed by PV cells are not able to convert into electricity, some of them are increase temperature, thus the performance varied. As discussed in this book chapter, most of the study showed that summer months when irradiation becomes high that leads to an increase of module temperature, a-Si technology show better performance than c-Si PV modules. It may be due to the metastable defects generated during the dangling bond compensation are decreased upon module temperature increase and as a result, the module performs better in elevated temperature. Also, CIGS PV modules show similar behavior to the a-Si PV modules. The performance gain observed in CIGS technology in summer or at elevated temperatures may be related to the larger bandgap and lower temperature coefficient. Particularly, the optical bandgap of CIGS thin film is higher than a-Si and the higher bandgap has a lower temperature coefficient. Also, CIGS modules can convert the blue light part of the solar spectrum due to a larger bandgap that may assist to perform better in hot summer. Alternatively, c-Si have a narrow bandgap, as the defect density increases upon high irradiance and high temperature in hot summer, the dark saturation current and/or leakage current is increased. Consequently, the performance decrease in summer.

However, it has been seen that c-Si perform very in high irradiance with cold weather. It should be noticed that the module with a higher leakage current is highly affected by low irradiance. Since a-Si solar cells inherently have high defect density and/or high leakage current than c-Si solar cells, thus the power gain by c-Si at very low irradiance is significantly higher than a-Si as discussed in the above section. Overall, CdTe modules are performed much poorer than others probably due to the consequence of early degradation of the module as reported in the previous section. All these above-mentioned studies specify the difficulty of choosing an appropriate PV technology for a given site. Thus, the prediction of PV energy potentials before installation is very important concerning the economic advantages and for policy regulation for electric utilities.

Acknowledgements

The authors wish to thank the Ministry of Higher Education of Malaysia (MoHE) for providing the Long Term Research Grant Scheme (LRGS) with the code of LRGS/1/2019/UKM-UNITEN/6/2 to support this research. The authors also acknowledge the publication support from the iRMC of Universiti Tenaga Nasional (@UNITEN), Malaysia. The authors would also like to acknowledge the Faculty of Engineering, University of Malaya (@UM) for other supports.

Author details

Mohammad Aminul Islam^{1,2*}, Nabilah M. Kassim^{2,3}, Ammar Ahmed Alkahtani^{2,3} and Nowshad Amin^{2,3}


1 Department of Electrical Engineering, Faculty of Engineering, University of Malaya, Jalan Universiti, Kuala Lumpur, Selangor, Malaysia

2 Institute of Sustainable Energy, Universiti Tenaga Nasional (@The Energy University), Jalan IKRAM-UNITEN, Kajang, Selangor, Malaysia

3 College of Engineering, Universiti Tenaga Nasional (@The Energy University), Jalan IKRAM-UNITEN, Kajang, Selangor, Malaysia

*Address all correspondence to: aminul.islam@um.edu.my

IntechOpen

© 2021 The Author(s). Licensee IntechOpen. This chapter is distributed under the terms of the Creative Commons Attribution License (<http://creativecommons.org/licenses/by/3.0>), which permits unrestricted use, distribution, and reproduction in any medium, provided the original work is properly cited. 

References

- [1] Ye, J.Y.; Reindl, T.; Aberle, A.G.; Walsh, T.M. Effect of solar spectrum on the performance of various thin-film PV module technologies in tropical Singapore. *IEEE J. Photovolt.* 2014, 4, 1268–1274.
- [2] Alonso-Abella, M.; Chenlo, F.; Nofuentes, G.; Torres-Ramirez, M. Analysis of spectral effects on the energy yield of different PV (photovoltaic) technologies: The case of four specific sites. *Energy* 2014, 67, 435–443.
- [3] Minemoto, T.; Nagae, S.; Takakura, H. Impact of spectral irradiance distribution and temperature on the outdoor performance of amorphous Si photovoltaic modules. *Solar Energy Mater. Solar Cells* 2007, 91, 919–923.
- [4] Gracia Amillo, A.; Huld, T.; Vourlioti, P.; Müller, R.; Norton, M. Application of satellite-based spectrally resolved solar radiation data to PV performance studies. *Energies* 2015, 8, 3455–3488.
- [5] Huld, T.A.; Friesen, G.; Skoczek, A.; Kenny, R.A.; Sample, T.; Field, M.; Dunlop, E.D. A power-rating model for crystalline silicon PV modules. *Solar Energy Mater. Solar Cells* 2011, 95, 3359–3369.
- [6] Huld, T.; Gottschalg, R.; Beyer, H.; Topić, M. Mapping the performance of PV modules, effects of module type and data averaging. *Solar Energy* 2010, 84, 324–338.
- [7] Koehl, M.; Heck, M.; Wiesmeier, S.; Wirth, J. Modeling of the nominal operating cell temperature based on outdoor weathering. *Solar Energy Mater. Solar Cells* 2011, 95, 1638–1646.
- [8] IEC Central Office. Photovoltaic Devices—Part 3: Measurement Principles for Terrestrial Photovoltaic (PV) Solar Devices with Reference Spectral Irradiance Data; Technical Report IEC 61215–3; International Electrotechnical Commission: Geneva, Switzerland, 2005.
- [9] World Bank. 2017. Global Solar Atlas. <https://globalsolaratlas.info>.
- [10] “RReDC Glossary of Solar Radiation Resource Terms”. rredc.nrel.gov. Retrieved 25 November 2017.
- [11] Kalogirou, Soteris, ed. McEvoy's handbook of photovoltaics: fundamentals and applications. Academic Press, 2017.
- [12] International Electro-Technical Commission. Standard IEC 60904–3: Photovoltaic Devices. Part 3: Measurement Principles for Terrestrial Photovoltaic (PV) Solar Devices With Reference Spectral Irradiance Data (Ed. 2, 2008)
- [13] Wikimedia Commons. (April 16, 2018). Solar Spectrum [Online]. Available: https://commons.wikimedia.org/wiki/File:Solar_Spectrum.png
- [14] Duffie JA, Beckman WA. Solar engineering of thermal processes. John Wiley&Sons Inc., Hoboken, New Jersey, 2006.
- [15] Hassanzadeh BH, de Keizer AC, Reich NH, van Sark WGJHM. The effect of a varying solar spectrum on the energy performance of solar cells. In: proceedings of 22nd European PVSEC, Milan, 2007. p. 2652–2658.
- [16] Ma, J., Man, K. L., Ting, T. O., Zhang, N., Guan, S. U., & Wong, P. W. (2013). Approximate single-diode photovoltaic model for efficient IV characteristics estimation. *The Scientific World Journal*, 2013.
- [17] Wu, N., Wu, Y., Walter, D., Shen, H., Duong, T., Grant, D., ... & Catchpole, K. (2017). Identifying the

cause of voltage and fill factor losses in perovskite solar cells by using luminescence measurements. *Energy Technology*, 5(10), 1827–1835.

[18] Luque A, Hegedus S. *Handbook of photovoltaic science and engineering*. John Wiley & Sons Inc., England, 2003.

[19] Gottschalg R, Betts TR, Infield DG, Kearney MJ, The effect of spectral variations on the performance parameters of single and double junction amorphous silicon solar cells. *Solar Energy Materials & Solar Cells* 2005; 85: 415–428.

[20] Shimokawa R, Miyake Y, Nakanishi Y, Kuouano Y, Hamakawa Y. Effect of atmospheric parameters on solar cell performance under global irradiance. *Solar Cells* 1986–1987; 19: 59–72.

[21] Rosell JI, Ibanez M, Modelling power output in photovoltaic modules for outdoor operating conditions. *Energy Conversion and Management* 2006; 47: 2424–2430.

[22] Sadok M, Mehdaoui A. Outdoor testing of photovoltaic arrays in the saharan region. *Renewable Energy* 2008; 33: 2516–2524.

[23] Kenny RP, Ioannides A, Müllejans H, Zaaiman W, Dunlop ED. Performance of thin film PV modules. *Thin Solid Films* 2006; 511–512: 663–672.

[24] Shaltout, M.A.M., El-Nicklawy, M., Hassan, A., Rahoma, U., Sabry, M., 2000. The temperature dependence of the spectral and efficiency behavior of Si solar cell under low concentrated solar radiation. *Renew. Energy* 21, 445–458.

[25] Silvestre, S., Senti's, L., Castaner, L., 1999. A fast low-cost solar cell spectral response measurement system with accuracy indicator. *IEEE Trans. Instrum. Meas.* 48 (5), 944–948.

[26] Makrides G, Zinsser B, Phinikarides A, Schubert M, Georghiou GE. Temperature and thermal annealing effects on different photovoltaic technologies. *Renewable Energy* 2012; 43: 407–417.

[27] Jiang JA, Wang JC, Kuo KC, Su YL, Shieh JC, Chou JJ. Analysis of the junction temperature and thermal characteristics of photovoltaic modules under various operation conditions. *Energy* 2012; 44: 292–301.

[28] Kamkird P, Ketjoy N, Rakwichian W, Sukchai S. Investigation on temperature coefficients of three types photovoltaic module technologies under Thailand operating condition. *Procedia Engineering* 2012; 32: 376–383.

[29] Mekhilef S, Saidur R, Kamalisarvestani M. Effect of dust, humidity and air velocity on efficiency of photovoltaic cells. *Renewable and Sustainable Energy Reviews* 2012; 16: 2920–2925.

[30] Singh P, Ravindra NM. Temperature dependence of solar cell performance-an analysis. *Solar Energy Materials & Solar Cells* 2012; 101: 36–45.

[31] Okullo W, Munji MK, Vorster FJ, van Dyk EE. Effects of spectral variation on the device performance of copper indium diselenide and multi-crystalline silicon photovoltaic modules. *Solar Energy Materials & Solar Cells* 2011; 95: 759–764.

[32] Dirnberger D, Blackburn G, Müller B, Reise C. On the impact of solar spectral irradiance on the yield of different PV technologies. *Solar Energy Materials and Solar Cells* 2015; 132: 431–442.

[33] Alonso-Abella M, Chenlo F, Nofuentes G, Torres- Ramírez M. Analysis of spectral effects on the energy yield of different PV (photovoltaic) technologies: the case of

- four specific sites. *Energy* 2014; 67: 435–443.
- [34] Nofuentes G, García-Domingo B, Muñoz JV, Chenlo F. Analysis of the dependence of the spectral factor of some PV technologies on the solar spectrum distribution. *Applied Energy* 2014; 113: 302–309.
- [35] Huld T, Amillo AMG. Estimating PV module performance over large geographical regions: the role of irradiance, air temperature, wind speed and solar spectrum. *Energies* 2015; 8(6): 5159–5181.
- [36] Ishii T, Otani K, Itagaki A, Utsunomiya K. A simplified methodology for estimating solar spectral influence on photovoltaic energy yield using average photon energy. *Energy Science & Engineering* 2013; 1(1): 18–26.
- [37] Cornaro C, Andreotti A. Influence of average photon energy index on solar irradiance characteristics and outdoor performance of photovoltaic modules. *Progress in Photovoltaics: Research and Applications* 2013; 21(5): 996–1003.
- [38] Betts TR, Jardine CN, Gottschalg R, Infield DG, Lane K. Impact of spectral effects on the electrical parameters of multijunction amorphous silicon cells, In *Proceedings of 3rd World Conference on Photovoltaic Energy Conversion*, 2003, 2003; 1756–1759.
- [39] Ishii T, Otani K, Itagaki A, Utsunomiya K. A methodology for estimating the effect of solar spectrum on photovoltaic module performance by using average photon energy and a water absorption band. *Japanese Journal of Applied Physics* 2012; 51: 51(10NF05).
- [40] Beard, M. C., Johnson, J. C., Luther, J. M., & Nozik, A. J. Multiple exciton generation in quantum dots versus singlet fission in molecular chromophores for solar photon conversion. *Philosophical Transactions of the Royal Society A: Mathematical, Physical and Engineering Sciences*, 2015; 373(2044): 20140412.
- [41] Minnaert, B., & Veelaert, P. A proposal for typical artificial light sources for the characterization of indoor photovoltaic applications. *Energies*, 2014; 7(3): 1500–1516.
- [42] Wild, M.; Folini, D.; Henschel, F.; Fischer, N.; Müller, B. Projections of long-term changes in solar radiation based on CMIP5 climate models and their influence on energy yields of photovoltaic systems. *Sol. Energy*, 2015; 116: 12–24.
- [43] R. Gottschalg, M. Rommel, D. G. Infield, Variation of solar cell equivalent circuit parameters under different operating conditions, in: *Proceedings of the 14th European Photovoltaic Solar Energy Conference*, WIP-Munich, Barcelona, 1997, pp.2176–2179.
- [44] Hubin, J., & Shah, A. V. Effect of the recombination function on the collection in a p–i–n solar cell. *Philosophical Magazine B*, 1995; 72(6): 589–599.
- [45] Huld, T., Gottschalg, R., Beyer, H. G., & Topič, M. Mapping the performance of PV modules, effects of module type and data averaging. *Solar Energy*, 2010; 84(2): 324–338.
- [46] Gottschalg, R., Betts, T. R., Eeles, A., Williams, S. R., & Zhu, J. Influences on the energy delivery of thin film photovoltaic modules. *Solar energy materials and solar cells*, 2013; 119: 169–180.
- [47] Colle S, De Abreu, SL, Ruther R. Uncertainty in economic analysis of solar water heating and photovoltaic systems. *Solar Energy*, 2001; 70(2): 131–142.
- [48] Prentice, J.S.C. Spectral response of a-Si:H p-i-n solar cells. *Sol. Energy Mater. Sol. Cells* 2001; 69: 303–314.

- [49] Dirnberger, D.; Blackburn, G.; Muller, B.; Reise, C. On the impact of solar spectral irradiance on the yield of different PV technologies. *Sol. Energy Mater. Sol. Cells* 2015; 132: 431–442.
- [50] Tsao, J., Lewis, N. and Crabtree, G. Solar faqs. US department of Energy, 13, 2006.
- [51] Nann, S.; Emery, K. Spectral effects on PV-device rating. *Sol. Energy Mater. Sol. Cells* 1992; 27: 189–216.
- [52] Eke, R.; Betts, T.R.; Gottschalg, R. Spectral irradiance effect on the outdoor performance of photovoltaic modules. *Renew. Sustain. Energy Rev.* 2017; 69: 429–434.
- [53] Bird, R.E. A simple, solar spectral model for direct-normal and di use horizontal irradiance. *Sol. Energy* 1984; 32: 461–471.
- [54] McClatchey, R.A.; Selby, J.E. Atmospheric Transmittance from 0.25 to 28.5 μm : Computer Code LOWTRAN2; AFCRL-72-0745, Environ. Res. Paper No. 427; Airforce Cambridge Research Laboratories: Wright-Patterson Air Force Base, OH, USA, 1972.
- [55] Gueymard, C.A. REST2, High-performance solar radiation model for cloudless-sky irradiance, illuminance, and photosynthetically active radiation—Validation with a benchmark dataset. *Sol. Energy* 2008; 82: 272–285.
- [56] Gueymard, C.A. SMARTS2, a Simple Model. of the Atmospheric Radiative Transfer of Sunshine: Algorithms and Performance Assessment; FSEC-PF-270-95; Florida Solar Energy Center: Cocoa, FL, USA, 1995.
- [57] Gueymard, C.A., REST2: High-performance solar radiation model for cloudless-sky irradiance, illuminance, and photosynthetically active radiation—Validation with a benchmark dataset. *Solar Energy*, 2008; 82(3): 272–285.
- [58] Utrillas, M.P., Bosca, J.V., Martínez-Lozano, J.A., Cañada, J., Tena, F. and Pinazo, J.M. A comparative study of SPCTRAL2 and SMARTS2 parameterised models based on spectral irradiance measurements at Valencia, Spain. *Solar energy*, 1998; 63(3): 161–171.
- [59] Gueymard, C.A. Interdisciplinary applications of a versatile spectral solar irradiance model: A review. *Energy*, 2005; 30(9): 1551–1576.
- [60] Myers, D.R., Emery, K. and Gueymard, C. Revising and validating spectral irradiance reference standards for photovoltaic performance evaluation. *J. Sol. Energy Eng.*, 2004; 126(1): 567–574.
- [61] Philipps, S.P., Peharz, G., Hoheisel, R., Hornung, T., Al-Abbadi, N.M., Dimroth, F. and Bett, A.W. Energy harvesting efficiency of III–V triple-junction concentrator solar cells under realistic spectral conditions. *Solar Energy Materials and Solar Cells*, 2010; 94(5): 869–877.
- [62] Jaus, J. and Gueymard, C.A. Generalized spectral performance evaluation of multijunction solar cells using a multicore, parallelized version of SMARTS. In AIP Conference Proceedings, 2012; 1477(1): 122–126).
- [63] Marion, B. Preliminary investigation of methods for correcting for variations in solar spectrum under clear skies, 2010.
- [64] Guechi, A. and Chegaar, M. Effects of diffuse spectral illumination on microcrystalline solar cells. *J. Electron Devices*, 2007; 5: 116–121.
- [65] Dobbin, A., Norton, M., Georghiou, G.E., Lumb, M. and Tibbits, T.N. December. Energy harvest predictions

for a spectrally tuned multiple quantum well device utilising measured and modelled solar spectra. In AIP Conference Proceedings, 2011; 1407(1): 21–24).

[66] Muller, M., Marion, B., Kurtz, S. and Rodriguez, J. An investigation into spectral parameters as they impact CPV module performance. In AIP conference proceedings, 2010; 1277(1): 307–311).

[67] Gueymard, C.A., The sun's total and spectral irradiance for solar energy applications and solar radiation models. *Solar energy*, 2004; 76(4): 423–453.

[68] Monokroussos, C., Zhang, X. Y., Schweiger, M., Etienne, D., Liu, S., Zhou, A., ... & Zou, C. (2017). Energy Rating of c-Si and mc-Si Commercial PV-Modules in Accordance with IEC 61853–1,-2,-3 and Impact on the Annual Yield. In Proceedings of 33rd European Photovoltaic Solar Energy Conference.

[69] Habibi, M., Zabihi, F., Ahmadian-Yazdi, M. R., & Eslamian, M. (2016). Progress in emerging solution-processed thin film solar cells–Part II: Perovskite solar cells. *Renewable and Sustainable Energy Reviews*, 62, 1012–1031.

[70] Zhang, C., Shen, H., Sun, L., Yang, J., Wu, S., & Lu, Z. (2020). Bifacial p-Type PERC Solar Cell with Efficiency over 22% Using Laser Doped Selective Emitter. *Energies*, 13(6), 1388.

[71] Zhao, J., Wang, A., & Green, M. A. (2001). High-efficiency PERL and PERT silicon solar cells on FZ and MCZ substrates. *Solar Energy Materials and Solar Cells*, 65(1–4), 429–435.

[72] Vasudevan, R., Harrison, S., D'Alonzo, G., Moustafa, A., Nos, O., Muñoz, D., & Roux, C. (2018, August). Laser-induced BSF: A new approach to simplify IBC-SHJ solar cell fabrication. In AIP Conference Proceedings (Vol. 1999, No. 1, p. 040024). AIP Publishing LLC.

[73] A. F. Panchula et al., “First year performance of a 20 MWac PV power plant,” in 37th IEEE Photovoltaic Specialists Conference (PVSC) (2011).

[74] A. Dolara et al., “Performance analysis of a single-axis tracking PV system,” *IEEE J. Photovolt.* 2(4), 524–531 (2012).

[75] Romero-Fiances, I., Muñoz-Cerón, E., Espinoza-Paredes, R., Nofuentes, G., & De la Casa, J. (2019). Analysis of the performance of various pv module technologies in Peru. *Energies*, 12(1), 186.

[76] Kazem, H.A.; Khatib, T.; Sopian, K.; Elmenreich, W. Performance and feasibility assessment of a 1.4 kW roof top grid-connected photovoltaic power system under desertic weather conditions. *Energy Build.* 2014, 82, 123–129

[77] Fuentes, M.; Nofuentes, G.; Aguilera, J.; Talavera, D.L.; Castro, M. Application and validation of algebraic methods to predict the behaviour of crystalline silicon PV modules in Mediterranean climates. *Sol. Energy* 2007, 81, 1396–1408.

[78] Muñoz, J.V.; Nofuentes, G.; Fuentes, M.; de la Casa, J.; Aguilera, J. DC energy yield prediction in large monocrystalline and polycrystalline PV plants: Time-domain integration of Osterwald's model. *Energy* 2016, 114, 951–960.

[79] Bahaidarah, H., Rehman, S., Subhan, A., Gandhidasan, P., & Baig, H. (2015). Performance evaluation of a PV module under climatic conditions of Dhahran, Saudi Arabia. *Energy exploration & exploitation*, 33(6), 909–929.

[80] Edalati, S.; Ameri, M.; Iranmanesh, M. Comparative performance investigation of mono- and polycrystalline silicon photovoltaic modules for use in grid-connected photovoltaic systems in dry climates. *Appl. Energy* 2015, 160, 255–265.

- [81] Ghitas, A. E. (2012). Studying the effect of spectral variations intensity of the incident solar radiation on the Si solar cells performance. *NRIAG Journal of Astronomy and Geophysics*, 1(2), 165–171.
- [82] Eke, R.; Demircan, H. Performance analysis of a multi crystalline Si photovoltaic module under Mugla climatic conditions in Turkey. *Energy Convers. Manag.* 2013, 65, 580–586.
- [83] Bora, B.; Kumar, R.; Sastry, O.S.; Prasad, B.; Mondal, S.; Tripathi, A.K. Energy rating estimation of PV module technologies for different climatic conditions. *Sol. Energy* 2018, 174, 901–911.
- [84] N. J. Reich et al., “Crystalline silicon cell performance at low light intensities,” *Sol. Energy Mater. Sol. Cells* 93(9), 1471–1481 (2009)
- [85] Chander, S., Purohit, A., Sharma, A., Nehra, S. P., & Dhaka, M. S. (2015). Impact of temperature on performance of series and parallel connected mono-crystalline silicon solar cells. *Energy Reports*, 1, 175–180.
- [86] Atsu, D., & Dhaundiyal, A. (2019). Effect of Ambient Parameters on the Temperature Distribution of Photovoltaic (PV) Modules. *Resources*, 8(2), 107.
- [87] Pervaiz, S., & Khan, H. A. (2015). Low irradiance loss quantification in c-Si panels for photovoltaic systems. *Journal of Renewable and Sustainable Energy*, 7(1), 013129.
- [88] Cotfas, D. T., & Cotfas, P. A. (2019). Comparative Study of Two Commercial Photovoltaic Panels under Natural Sunlight Conditions. *International Journal of Photoenergy*, 2019.
- [89] Gaglia, A.G.; Lykoudis, S.; Argiriou, A.A.; Balaras, C.A.; Dialynas, E. Energy efficiency of PV panels under real outdoor conditions—An experimental assessment in Athens, Greece. *Renew. Energy* 2017, 101, 236–243
- [90] Luceño-Sánchez, J. A., Díez-Pascual, A. M., & Peña Capilla, R. (2019). Materials for photovoltaics: State of art and recent developments. *International journal of molecular sciences*, 20(4), 976.
- [91] Shafarman, W.N.; Stolt, L. Cu (InGa)Se₂ solar cells. In *Handbook of Photovoltaic Science and Engineering*; Luque, A., Hegedus, S., Eds.; Wiley: Hoboken, NJ, USA, 2003; pp. 567–616.
- [92] Khana, N.A.; Rahmanb, K.S.; Aris, K.A.; Ali, A.M.; Misran, H.; Akhtaruzzaman, M.; Tiong, S.K.; Amin, N. Effect of laser annealing on thermally evaporated CdTe thin films for photovoltaic absorber application. *Sol. Energy* 2018, 173, 1051–1057.
- [93] Islam, M. A., Rahman, K. S., Sobayel, K., Enam, T., Ali, A. M., Zaman, M., ... & Amin, N. (2017). Fabrication of high efficiency sputtered CdS: O/CdTe thin film solar cells from window/absorber layer growth optimization in magnetron sputtering. *Solar Energy Materials and Solar Cells*, 172, 384–393.
- [94] Morigaki, K.; Ogihara, C. Amorphous Semiconductors: Structure, Optical and Electrical Properties. In *Springer Handbook of Electronic and Photonic Materials*; Kasap, S., Capper, P., Eds.; Springer: Cham, Germany, 2017.
- [95] Gulkowski, S., Zdyb, A., & Dragan, P. (2019). Experimental efficiency analysis of a photovoltaic system with different module technologies under temperate climate conditions. *Applied Sciences*, 9(1), 141.
- [96] Gottschalg, R.; Betts, T.R.; Eeles, A.; Williams, A.R.; Zhu, J. Influences on the energy delivery of thin film photovoltaic modules. *Sol. Energy Mater. Sol. Cells* 2013, 119, 169–180.

- [97] Louwen, A.; de Waal, A.C.; Schropp, R.E.I.; Faaij, A.P.C.; van Sark, W.G.J.H.M. Comprehensive characterization and analysis of PV module performance under real operating conditions. *Prog. Photovolt. Res. Appl.* 2017, 25, 218–232.
- [98] Ozden, T., Akinoglu, B. G., & Turan, R. (2017). Long term outdoor performances of three different on-grid PV arrays in central Anatolia—An extended analysis. *Renewable energy*, 101, 182–195.
- [99] Kesler, S.; Kivrak, S.; Dincer, F.; Rustemli, S.; Karaaslan, M.; Unal, E.; Erdiven, U. The analysis of PV power potential and system installation in Manavgat, Turkey—A case study in winter season. *Renew. Sustain. Energy Rev.* 2014, 31, 671–680.
- [100] Sharma, V.; Kumar, A.; Sastry, O. S.; Chandel, S.S. Performance assessment of different solar photovoltaic technologies under similar outdoor conditions. *Energy* 2013, 58, 511–518.
- [101] Makrides G, Zinsser B, Phinikarides A, Schubert M, Georghiou GE. Temperature and thermal annealing effects on different photovoltaic technologies. *Renewable Energy* 2012;43:407e17.
- [102] Aste, N.; Del Pero, C.; Leonforte, F. PV technologies performance comparison in temperate climates. *Sol. Energy* 2014, 109, 1–10.
- [103] Louwen, A.; de Waal, A.C.; Schropp, R.E.I.; Faaij, A.P.C.; van Sark, W.G.J.H.M. Comprehensive characterization and analysis of PV module performance under real operating conditions. *Prog. Photovolt. Res. Appl.* 2017; 25: 218–232
- [104] Zdyb, A., & Gulkowski, S. (2020). Performance Assessment of Four Different Photovoltaic Technologies in Poland. *Energies*, 13(1), 196.
- [105] Minemoto, T., Toda, M., Nagae, S., Gotoh, M., Nakajima, A., Yamamoto, K., ... & Hamakawa, Y. (2007). Effect of spectral irradiance distribution on the outdoor performance of amorphous Si//thin-film crystalline Si stacked photovoltaic modules. *Solar Energy Materials and Solar Cells*, 91(2–3), 120–122.
- [106] Akhmad K, Kitamura A, Yamamoto F, Okamoto H, Takakura H, Hamakawa Y. Outdoor performance of amorphous silicon and polycrystalline silicon PV modules. *Solar Energy Materials and Solar Cells* 1997; 46(3): 209–218.
- [107] Nishioka, K., Hatayama, T., Uraoka, Y., Fuyuki, T., Hagihara, R., & Watanabe, M. (2003). Field-test analysis of PV system output characteristics focusing on module temperature. *Solar Energy Materials and Solar Cells*, 75(3–4), 665–671.
- [108] Poissant, Y. (2009, June). Field assessment of novel PV module technologies in Canada. In *Proc. 4th Canadian Solar Buildings Conference*, June.
- [109] Cañete, C., Carretero, J., & Sidrach-de-Cardona, M. (2014). Energy performance of different photovoltaic module technologies under outdoor conditions. *Energy*, 65, 295–302.
- [110] Maluta, E., & Sankaran, V. (2011). Outdoor testing of amorphous and crystalline silicon solar panels at Thohoyandou. *Journal of Energy in Southern Africa*, 22(3), 16–22.
- [111] Shaltout, M. M., El-Hadad, A. A., Fadly, M. A., Hassan, A. F., & Mahrous, A. M. (2000). Determination of suitable types of solar cells for optimal outdoor performance in desert climate. *Renewable energy*, 19(1–2), 71–74.